Proceedings of the 16th International Conference on Soil Mechanics and Geotechnical Engineering

doi:10.3233/978-1-61499-656-9-1667

Ground and lining responses during tunnelling in saturated ground – 3D stress-pore pressure coupled analysis

Les réponses du sol et du lining pendant la construction du tunnel en sol saturé-L'analyse couplée de l'effort 3D-la pression de pore

C. Yoo & S. B. Kim
Dept. of Civil and Envir. Engrg., Sungkyunkwan University, Suwon, Korea

ABSTRACT

Construction of a tunnel in urban area has become increasingly challenging due to the increased public concern regarding the impact of tunnelling on surrounding environments. In this regards, the control of groundwater has become an essential part of the planning, design, and construction of a tunnelling project. This paper presents the results of an investigation on interaction mechanism between tunnelling and groundwater using a 3D stress-pore pressure coupled finite-element model. It is shown that the ground and lining responses are significantly influenced by the relative permeability of the lining, and that the circumferential pregrouting is an effective means for minimizing the tunnelling and groundwater interaction.

RÉSUMÉ

La construction d'un tunnel et son entretien dans la zone urbain devient de plus en plus difficile au fur et à mesure que le public s'intéresse et s'inquiète davantage en ce qui concerne l'effet de la construction du tunnel aux environnements. Pour cette raison, le contrôle de l'eau souterraine devient importante pour le projet, le dessin et la construction du tunnel. Dans cette thèse, nous avons examiné le méchanisme de l'interaction entre la construction du tunnel et l'eau souterraine en exerçant "3D stress-pore pressure coupled finite-element model". Ces recherches nous ont montré que les réponses du sol et du "lining" est principalement influencées par l'imperméabilité du "lining" et le "pre-grouting" des environs du tunnel est efficace pour minimiser l'interaction de la construction du tunnel et l'eau souterrain

1 INTRODUCTION

As urban population continues to grow, there has been a pressing need for construction of new tunnels for transportation systems and underground utilities. Due to the increased public awareness on the impact of tunnelling on surrounding environments, however, construction of urban tunnels are becoming increasingly challenging. A good example is the construction project for new Seoul Subway Line 9 (Contract 912), that is being constructed in Seoul, Korea (Figure 1). The entire construction project runs across west and east parts of Seoul, along Han River, and consists of cut and cover sections as well as drill and blast tunnel sections. One example of difficult tunnelling conditions being encountered is illustrated Figure 1(b). The initial design, as seen in this figure, requires that a 10 m diameter tunnel be constructed partly through a water bearing alluvial layer consisting of predominantly fine sands directly under an existing expressway, requiring cutting parts of existing piles. Apart from the interaction between the expressway and tunnelling, concerns are raised on the effects of groundwater and tunnelling interaction on the tunnelling performance. In such situations, it is essential to understand principles of the effect of tunnelling and groundwater interaction on the tunnelling performance in order to provide optimum mitigation measures, if necessary.

Despite the importance of understanding the effect of tunneling and groundwater interaction on tunnelling performance, studies concerning this subject are limited. Some of the available studies related to this subject focused more or less on the hydrodynamic nature of the problem dealing with the influence of the seepage flow towards the tunnel (Schweiger et al. 1991; Katzenbach 1995), and of the lowering of the water table (Adachi et al. 1988) on the stability of the opening and on the loads carried by its liner. Other studies of similar nature are specifically related to the effects of tunnelling on the groundwater regime in the surrounding medium (Daito and Ueshita 1988; Ueshita and Daito 1985). Gunn and Talyor (1984), Atwa and Leca (1994), Pottler et al. (1994) and Schweiger et al. (1999) have performed numerical analyses on the problem similar to that addressed in this study, but with the steady-state seepage analysis or sequential seepage analysis and stress analysis, which can not accurately model the fully

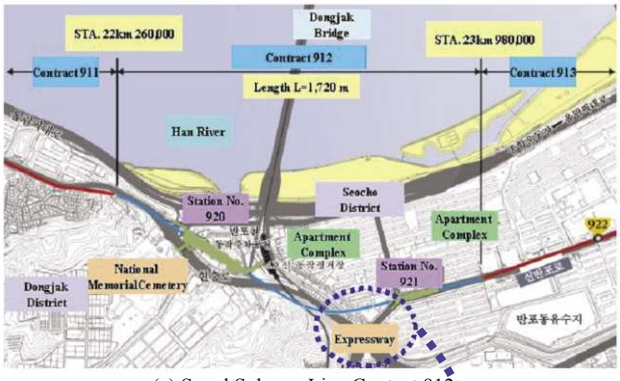

(a) Seoul Subway Line Contact 912

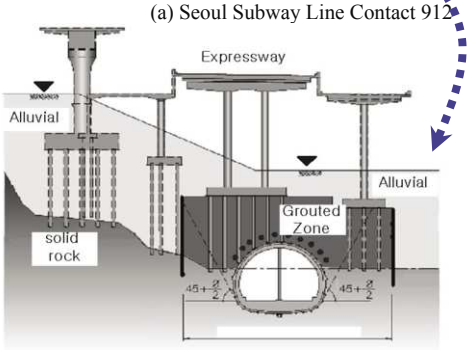

(b) One example of difficult section

Figure 1. An example of difficult tunnelling condition in Seoul Metro Subway Line 9 construction project

coupled interaction behavior between the tunnelling and the groundwater. More recent studies include those by Shin et al. (2002a, b) in which the effect of ground water on the long-term tunnel behavior was studied using a plane strain and an axisymmetric finite-element models.

As part of a pre-investigation on the tunnelling conditions of the Seoul Metro Subway construction project aiming at reviewing initial designs and establishing construction guidelines, a parametric study was performed on various factors affecting the tunnelling performance using a fully coupled 3D finite-element model. This paper presents the 3D finite-element model, simulation strategy, and finally, practical implications of the findings.

2 PRAMETRIC STUDY

2.1 *Tunnelling condition*

A parametric study using a 3D finite-element model was performed on a typical 10-m-diameter horseshoe shaped tunnel constructed 25 m below the ground surface in the ground condition frequently encountered in Seoul, Korea. Figure 2 shows the ground profile considered in this study. The tunnel is excavated through a moderately weathered granite rock layer of Grade III, according to the engineering classification of weathered rock (Waltham 1994). For simplicity, the groundwater table was assumed to be located at the ground surface level. In regard to the post-tunnelling groundwater flow regime, a drawdown condition with no recharge at the ground surface during the tunnelling process was assumed. Such a post-tunnelling groundwater flow condition was purposely selected to look into rather extreme cases in terms of the groundwater drawdown, although one can argue that in reality such a condition is only valid during a very dry season as there usually exists near-surface recharge from leaking water pipes in urban conditions.

The tunnel is assumed to be constructed using the conventional drill and blast technique with a 30 cm thick shotcrete lining. Although rock bolts are usually installed as part of the primary support in this type of tunnelling condition, no rock bolts were considered for the sake of modeling simplicity.

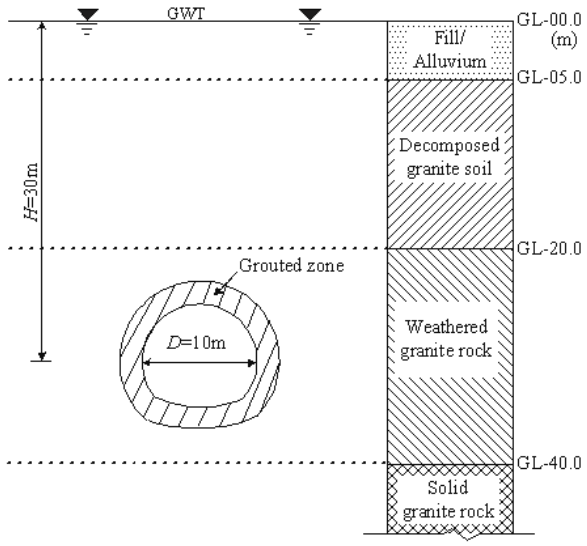

Figure 2. Ground profile for tunnelling condition analyzed

2.2 *Finite-element model*

In order to realistically capture the interaction mechanism between the tunnelling and the groundwater, a fully coupled 3D finite-element model capable of simulating the sequential tunnelling process was adopted for analyses. For analysis, a commercial finite-element package *ABAQUS* (*ABAQUS users manual* 2002) was used. The tunnel was assumed to be excavated full face, and therefore, only one half of the domain was considered in the finite-element model by making use of the symmetry about the tunnel centerline. The finite-element mesh extends to a depth of two times the tunnel diameter (D) below the tunnel springline and laterally to a distance of 8.0D from the tunnel centerline. Appropriate hydraulic boundary conditions are also prescribed in the model.

The ground was discretized using eight-node trilinear displacement and pore pressure elements with reduced integration (C3D8RP), while the shotcrete lining was modeled using four-node doubly curved general-purpose shell elements with reduced integration with hourglass control and finite membrane strains (S4R). The finite permeability of the shotcrete lining was simulated based on the approach by Shin et al. (2002a), in which shell elements are combined with continuum elements having a prescribed permeability. For those cases with pregrouting, the grouting effect is modeled by changing the material properties to those of the grouted zone at designated steps. In the analysis, the soil and rock layers were assumed to be an elasto-plastic material conforming to the extended Drucker-Prager failure criterion together with the nonassociated flow rule, while the shotcrete was assumed to behave in a linear elastic manner. Table 1 shows the material properties for the ground.

Table 1. Material properties used.

Material	c' (kPa)	ϕ' (°)	ψ (°)	k (m/sec)	E (MPa)	K_o
Fill	5	30	20	2×10^{-6}	30	0.4
Decomposed granite soil	50	38	15	1×10^{-6}	70	0.5
Weathered granite rock	100	40	15	6×10^{-7}	100	0.5
Solid Granite rock	200	45	15	1×10^{-9}	100	0.7
Grouted zone	200	50	10	6×10^{-9}	500	0.5
Shotcrete	-	-	-	1×10^{-8}	2000	-

In order to form a database that can help identify the interaction mechanism between the tunnelling and the groundwater, a number of cases were constructed by varying the permeability k_L/k_S of the lining relative to the ground through which the tunnel is excavated. In addition to k_L/k_S a number of cases with different pregrouting schemes with varying overlap length (L_G) between each grouting round were analyzed. For comparison, a total stress analysis with no consideration of the stress-pore pressure coupled effect was additionally conducted on the same tunnelling condition.

3 SHOTCRETE LINING RESPONSE

3.1 *General behavior*

The axial force distributions in the shotcrete lining are shown in Figure 3 for a section 2.0D behind the tunnel face. Normalized forces $T/\gamma' HD$ are presented in this figure, where T is the calculated shotcrete axial force per unit length of the tunnel drive and γ' is the average effective unit weight of the ground above the tunnel axis.

Four important trends can be observed in this figure. First, it is evident that the total stress analysis yields significantly smaller lining forces than the coupled analyses in some cases, especially at the invert, demonstrating that the lining forces can be significantly underestimated when performing a total stress analysis with no consideration of the stress-pore pressure coupled effect. Second, the variation in the lining forces with k_L/k_S tends to be more pronounced below the springline, thus suggesting that a special consideration be given to the invert stability when designing the lining for cases with smaller k_L/k_S. Third, no significant variation can be observed among the cases having a same k_L/k_S despite the differences in the level of the drawdown H_D. Fourth, for the finite lining permeability cases of $k_L = 1\times10^{-8} m/s$, in which two different relative lining permeability ratios are considered, i.e., $k_L/k_S = 0.2$ and 0.02, the lining forces for $k_L/k_S = 0.02$ are significantly greater than for $k_L/k_S = 0.2$, especially at the invert, although H_D for $k_L/k_S = 0.02$ is approximately three times larger than for $k_L/k_S = 0.2$. The results imply that the relative lining permeability k_L/k_S is a more important controlling factor in the development of lining forces than the post-tunnelling groundwater level, and that correct evaluation of the lining permeability is thus an important task in the context of lining design as it governs the actual pore water pressures acting on the lining.

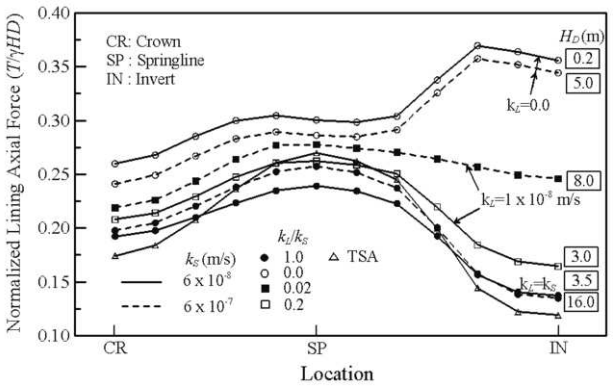

Figure 3. Variation of lining axial force with k_L/k_S

3.2 *Effect of* k_L/k_S

The effects of relative lining permeability ratio (k_L/k_S) and drawdown level (H_D) on the lining response are illustrated in different forms in Figure 4. Salient features shown in this figure are two fold. First, the axial lining force at the crown does not appear to be significantly influenced by k_L/k_S whereas there is a tendency for the lining force to decrease with increasing k_L/k_S at the invert. Second, no significant tie can be established between $T/\gamma' HD$ and H_D. Such results are in contrast to the current design practice in which design water pressures are selected based on the hydraulic head above the tunnel crown. Further study is required to establish the relationship between the drawdown level and the lining forces.

4 CIRCUMFERENTIAL PREGROUTING

4.1 *Effect on groundwater regime*

The effect of pregrouting on the groundwater regime and the tunnelling performance is examined for the case of $k_L/k_S = 0.02$. Four different overlap lengths L_G are considered, i.e., L_G=0.4D, 0.6D, 0.8D, and 1.0D. It should be noted that no solutions were obtained for cases $L_G < 0.4D$ due to numerical difficulties arising from the face instability, suggesting that $L_G = 0.4D$ is a critical overlap length below which the tunnel stability cannot be assured for the tunnelling condition considered in this study.

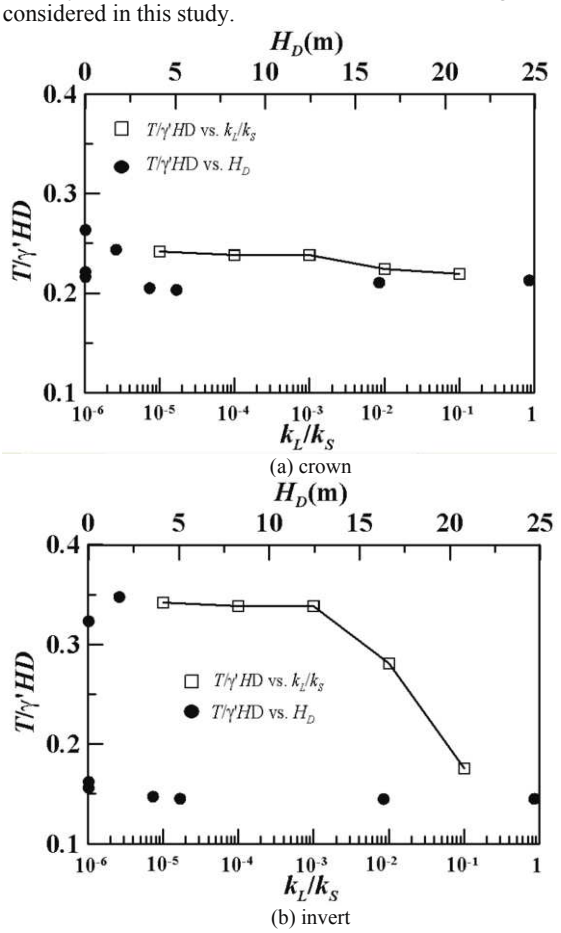

Figure 4. Variation of lining axial force with k_L/k_S and H_D: (a) crown; and (b) invert

Illustrated in Figure 5 are the pore water pressure distributions after the face advances to a distance 4.0D from the front boundary. Also shown in this figure is a table summarizing the magnitudes and extent of the drawdown for the cases analyzed. As seen in Figure 5, the pregrouting tends to significantly reduce the magnitude and the extent of the drawdown. In fact, the drawdown is kept below 1.8 m when employing the pregrouting with $L_G \geq 0.4D$ as opposed to 9 m for the case without the pregrouting. The lateral (X_D) and longitudinal (Y_D) extents of the drawdown zone are also reduced almost by half when adopting the pregrouting. With regard to the effect of L_G, it appears that the overlap length L_G does not appear to significantly influence the magnitude of the drawdown, exhibiting H_D=1.4~1.8 m for all cases. The longitudinal extent of the drawdown ahead of face (Y_D) is more influenced by L_G, showing a 30 % reduction when increasing L_G from 0.4D to 1.0D. The water pressures ahead of the face also decrease with increasing L_G, as illustrated in this figure.

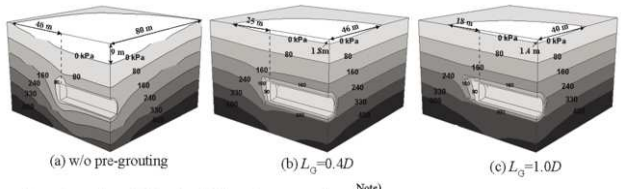

L_G	H_D (m)	X_D (m)	Y_D (m)
0.0D	9 m	80 m	40 m
0.4D	1.8 m	46 m	25 m
0.8D	1.6 m	44 m	20 m
1.0D	1.4 m	40 m	18 m

Note)
L_G = longitudinal extent of grouting ahead of face
H_D = drawdown
X_D = lateral extent of drawdown
Y_D = longitudinal extent of drawdown ahead of face
L_G = 0.0D indicates no pre-grouting.

Figure 5. Pore-water distributions for with and w/o pregrouting: (a) w/o pregrouting; (b) L_G=0.4D; and (c) L_G=1.0D

4.2 *Effect on ground and face deformations*

The positive effect of the pregrouting on the ground settlements and the face displacements is well illustrated in Figure 6. As seen in Figure 6(a), the settlement troughs for the pregrouting cases are considerably narrower and shallower, showing a maximum settlement of 13 mm as opposed to 70 mm for the case without the pregrouting. As for the drawdown, the overlap length L_G appears to have insignificant effect on the surface settlements, showing the maximum values in the range of 8~13 mm for $L_G = 0.4 \sim 1.0D$. The reduced settlements are mainly attributed to the decreased level of groundwater drawdown, although the umbrella effect by the grouted zone ahead of the face also provides a positive effect. It should be noted that pregrouting provides an umbrella effect that reduces the earth load ahead of the face, thus promoting the face stability. The pregrouting is also effective in reducing the face axial displacements as seen in Figure 6(b). One important observation is that when $L_G = 0.4D$, the face displacements are even larger than without the pregrouting. The increased pore water pressures ahead of the face and insufficient umbrella effect are mainly responsible for such a trend. Care should thus be exercised when selecting the overlap length L_G to avoid the face instability problem. In addition, no further benefit in terms of reducing the face displacement is apparent when $L_G > 0.6D$. Considering the repetitive nature of the grouting work, the threshold value of $L_G = 0.6D$ can be regarded as an optimum overlap length $L_{G,opt}$ required between two successive cycles, since any shorter length would yield rather large face and ground deformations.

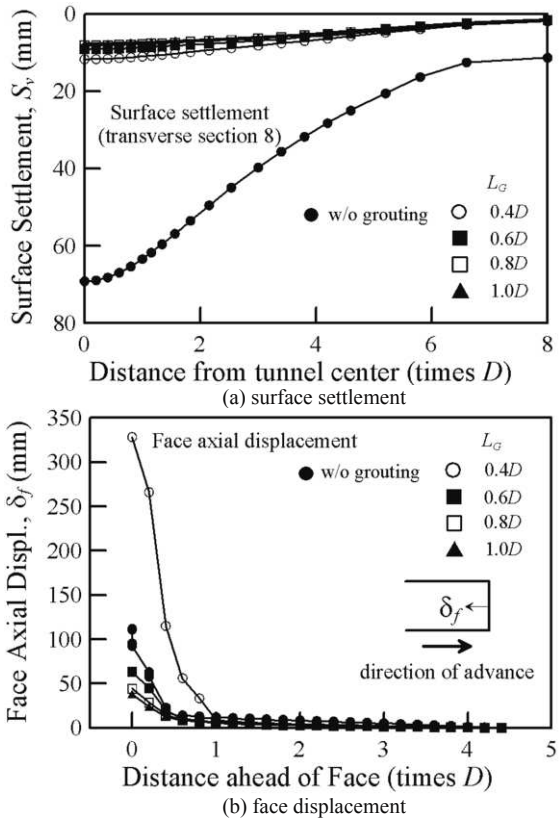

(a) surface settlement

(b) face displacement

Figure 6. Effect of overlap length of pregrouting on ground deformation: (a) surface settlement and (b) face displacement

5 CONCLUSIONS

This paper examined the interaction mechanism between tunnelling and groundwater using the results from a series of 3D stress-pore water coupled analyses on a typical tunnelling condition encountered in the construction of Seoul Subway Line 9 in Korea. Attention was paid to analyzing the results so that the effect of relative lining permeability on the pore water pressure regime as well as the ground and lining responses could be identified. The effect of a pregrouting scheme was also analyzed. The results indicated that for a range of the relative lining permeability with respect to the ground permeability, the maximum shotcrete lining force varies by more than 200% depending upon the relative lining permeability. With regard to the circumferential pregrouting, the results of the findings indicated that an overlap length of $L_{G,opt} = 0.6D$ is required to obtain an optimum pregrouting benefit for tunnelling cases similar to that considered in this study.

ACKNOWLEDGEMENTS

This research is supported by Korea Ministry of Construction and Transportation under Grant No. C103A1000026-03A0200-02620. The financial support is greatly acknowledged.

REFERENCES

ABAQUS users manual, version 6.3. (2002). Hibbitt, Karlsson, and Sorensen, Inc., Pawtucket, Providence, R.I.

Adachi, T., Kikuchi, T., and Kimura, H. 1988. Behaviour and simulation of soil tunnel with thin cover. *Prof. 6th Int. Conf. on Numerical Methods in Geomechanics*, Innsbruck, 1585-1590.

Atwa, M. and Leca, E. 1994. Analysis of groundwater seepage into tunnels. *Proc. Int. congress on tunnelling and ground conditions*, Cairo, Egypt, 303-310.

Daito, K. and Ueshita, K. 1988. Prediction of tunnelling effects on groundwater condition by the water balance method. *Prof. 6th Int. Conf. on Numerical Methods in Geomechanics*, Innsbruck, 1585-1590.

Gunn, M. J. and Taylor, R. N. 1984. Discussion on Atkinson and Mair (1983). *Géotechnique* 35(1), 73-75.

Katzenbach, R. 1985. The influence of soil strength and water load to the safety of tunnel driving. *Prof. 5th Int. Conf. on Numerical Methods in Geomechanics*, Nagoya, 1207-1213.

Pottler, R., Hagemeister, A., Schweiger, H. F., and Faust, P. 1994. Influence of tunnel drive on groundwater level. *Proc. 8th Conf. of the Int. Association for Computer Methods and Advances in Geomechanics*, Morgantown, 1249-1258.

Schweiger, H. F., Pottler, R. K., and Steiner, H. 1991. Effects of seepage force on shotcrete lining of a large undersea cavern. *Proc. 7th Conf. of the Int. Association for Computer Methods and Advances in Geomechanics*, Cairns, 1503-1508.

Shin, J. H., Addenbrooke, T. I., and Potts, D. M. 2002a. A numerical study of the effect of groundwater movement on long-term tunnel behavior. *Géotechnique*, 52(6), 391-403.

Shin, J. H., Potts, D. M., and Addenbrooke, T. I. 2002b. Three-dimensional modeling of NATM tunnelling in decomposed granite soil. *Géotechnique*, 52(3), 187-200.

Schweger, H. F., Schuller, H., and Pottler, R. 1999. Some remarks on 2D models for numerical simulation of underground construction with complex cross-sections. *Proc. 9th Conf. of the. Association for Computer Methods and Advances in Geomechanics*, China, 1303-1308.

Ueshita, K., Sato, T, and Daito, K. 1985. Prediction of tunnelling effect on groundwater condition. *Prof. 5th Int. Conf. on Numerical Methods in Geomechanics*, Nagoya, 1215-1219.

Waltham, A. C. 1994. *Foundations of Engineering Geology*, Blackie Academic & Professional, London · Glasgow.